X-ray absorption for the study of warm dense matter

Plasma Phys. Control. Fusion **51** (2009) 124021 (9pp) doi:10.1088/0741-3335/51/12/124021

X-ray absorption for the study of warm dense matter

A Lévy[1], F Dorchies[1], M Harmand[1], C Fourment[1], S Hulin[1], O Peyrusse[1], J J Santos[1], P Antici[2], P Audebert[2], J Fuchs[2], L Lancia[2], A Mancic[2], M Nakatsutsumi[2], S Mazevet[3], V Recoules[3], P Renaudin[3] and S Fourmaux[4]

[1] Université de Bordeaux - CNRS - CEA, CELIA, Talence, F-33405 France
[2] LULI, Ecole Polytechnique, 91128 Palaiseau Cedex, France
[3] CEA-DIF, 91680 Bruyères-le-Châtel, France
[4] INRS-Energie et Matériaux, 1650 bd. L Boulet, J3X1S2 Varennes, Québec, Canada

Received 2 July 2009, in final form 24 August 2008
Published 11 November 2009
Online at stacks.iop.org/PPCF/51/124021

Abstract
A time-resolved ultrafast x-ray spectrometer is developed in order to extract the x-ray absorption near-edge spectroscopy (XANES) structure of an Al sample in the warm dense matter regime. In this context, an intense, broadband, short (ps) x-ray source based on the M-band emission from high-Z plasmas is optimized to maximize the photon flux around the Al K-edge. An experiment is reported, devoted to probe a solid Al foil isochorically heated by laser-produced protons up to 3 eV. The experimental x-ray spectra lead to an estimation of the electron temperature with an accuracy of 15%. In good agreement with two different theoretical approaches, the observed progressive smoothing of the XANES structures is clearly related to a significant loss of ion–ion correlation.

1. Introduction

The progress of science in the sub-picosecond domain pushed forward our understanding of the ultrafast dynamics in material structures [1]. Recently, there has been growing interest in the investigation of extreme states of matter such as the so-called warm dense matter (WDM) regime [2, 3]. This transient state is defined as the region in a phase diagram where the density ranges from the solid density up to 10 times its value and the temperature varies from 0.1 to 100 eV. This covers a wide panel of research areas including high-pressure physics, applied material studies, astrophysics, geophysics, inertial fusion as well as several industrial applications. The main difficulty in studying such a regime lies in its short lifetime which asks for time-resolved measurements with picosecond temporal resolution. In this state, the matter is partially correlated and degenerate and its complexity poses the numerical and theoretical modelling [4–6] a tremendous challenge. This requires the collection of new experimental data to discriminate between the theories and validate the models which are developed.

In this context, different techniques based on a 'pump–probe(x-ray)' scheme have been developed to extract structural information and properties of WDM states. Among the possible diagnostics, we can mention x-ray diffraction [7–10], x-ray scattering [11, 12], Thomson scattering [13–15] and absorption spectroscopy [16–22]. All these methods exploit various kinds of x-ray sources such as laser-induced plasma emission, harmonic radiation, x-ray diodes or synchrotron sources [1, 23]. The x-ray absorption fine spectroscopy (XAFS) is a particularly suited experimental technique to access structural information on a non-crystalline state of matter where short-range order dominates.

In this paper, we focus on the study of warm dense aluminium using ultrafast x-ray absorption near-edge spectroscopy (XANES). To extract the XANES spectra, we have optimized an ultrashort x-ray source maximizing the photon flux around the Al K-edge using the kilohertz laser system at the CEntre Lasers Intenses et Applications (CELIA) and developed a specific x-ray spectrometer. This diagnostic has been implemented on the experiment we have performed at the Laboratoire pour l'Utilisation des Lasers Intenses (LULI), devoted to probing the Al sample isochorically heated by protons. Measuring the absorption spectra, we access an accurate estimation of the electron temperature T_e and information on the local atomic structure of the sample [24]. These results are in good agreement with two different theoretical approaches modelling the warm dense regime of matter.

2. X-ray source and XANES diagnostic

In the first stage of this study, we have developed and optimized a suitable x-ray source in the energy range of the Al K-edge from 1.50 to 1.75 keV. For this purpose, we choose to take advantage of the intense broad M-band x-ray emission generated through the interaction of a short intense laser pulse with a high-Z target [25]. This preliminary study has been accomplished on the Aurore Ti : sapphire laser system at CELIA which delivers a 30 fs–5 mJ pulse at 1 kHz repetition rate.

Varying different laser parameters (duration, energy) and target material (Sm, Gd, Dy, Er and Yb), we maximized the broadband 4f–3d transition [26]. The x-ray conversion efficiency from the laser energy is about 10^{-3}, when integrated from 1.5 to 1.75 keV and over 2π sr. The duration of such a laser-based x-ray source varies from a few picoseconds for solid target, down to sub-picosecond with clusters [27].

To collect the transmitted spectra and deduce the absorption curves, we have developed a specific double x-ray spectrometer presented in figure 1(*a*). This device has been designed to record simultaneously the transmitted spectrum and the direct emission of the source coupling two conical KAP crystals. In this configuration, the results are released from shot-to-shot fluctuations. Both signals are focalized out of the plane of the detector (CCD or imaging plates) in order to obtain a spatial resolution in the same plane. The resulting XANES curve is plotted in figure 1(*b*), when probing a cold 1 μm thick Al sample and accumulating over 30 s at 1 kHz. It presents statistical fluctuations lower than 1% [28].

For the scope of the study presented in this paper, we extrapolated the optimal experimental conditions found at CELIA to optimize an x-ray source on the 100 TW laser facility at LULI (1 shot each 20 min). In agreement with this preliminary study, the maximal photon flux was obtained by the interaction of a 3 J–2.5 ps laser pulse with an erbium backlighter target. In addition, to enhance the signal-to-noise ratio, the laser pulse was frequency doubled by means of a non-linear crystal thus reducing the hard x-ray component and the induced background on the x-ray detector. The corresponding spectrum is reported in figure 1(*b*) that demonstrates the possibility of clearly resolving XANES structures in a single shot mode.

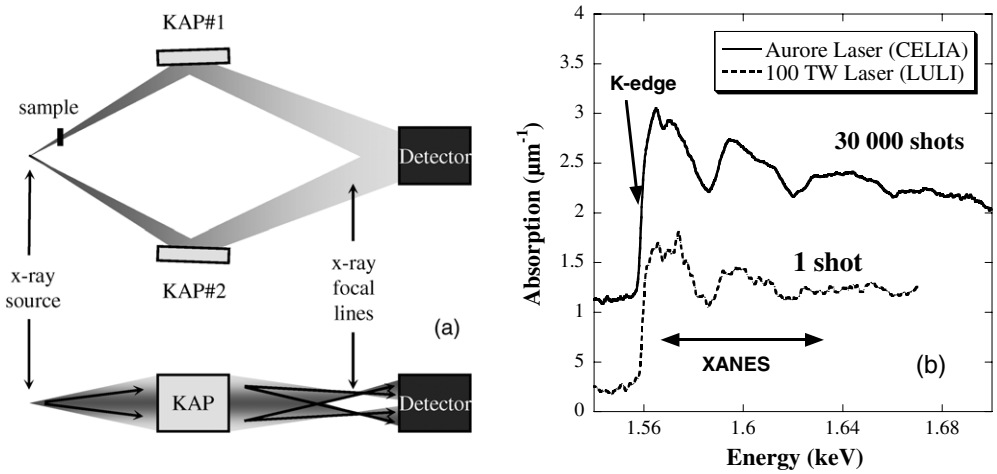

Figure 1. (*a*) Schematic of the double x-ray spectrometer. Both spectra are laterally shifted with respect to each other on the detector plane. (*b*) Typical absorption spectra of cold Al sample obtained on two different laser systems (artificially vertically shifted).

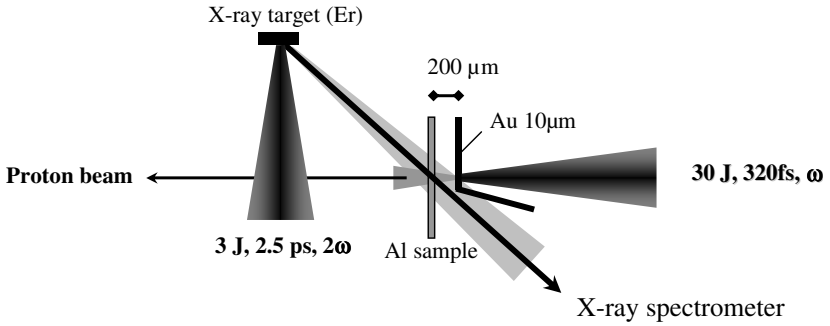

Figure 2. Schematic of the experimental set-up.

3. Protons isochoric heating of Al

3.1. Experimental set-up

The experiment has been performed at LULI using the 100 TW laser facility (central wavelength $\lambda_0 = 1.057\,\mu$m). A schematic representation of the set-up is reported in figure 2.

The main 320 fs laser pulse is focused at normal incidence onto a 10 μm thick Au primary target with an intensity of $\simeq 3 \times 10^{19}\,\mathrm{W\,cm^{-2}}$. Induced by this interaction, an energetic proton beam is generated at the rear side of the foil [29]. This short ($\simeq$ps), directional and laminar particle source [30] is devoted to isochorically heat the Al sample placed 200 μm behind the primary target. In this configuration, different studies have demonstrated the possibility of reaching an electron temperature around 10 eV at solid density [31–34] in a duration of about a few picoseconds. In this experiment, we varied the proton source and thus the sample heating by varying the laser focalization.

A delayed laser pulse with 3 J of energy in a 2.5 ps duration is focused on the backlighter Er target to generate the x-ray source. The absorption spectra obtained by the use of the double x-ray spectrometer described before have been collected for two different Al target

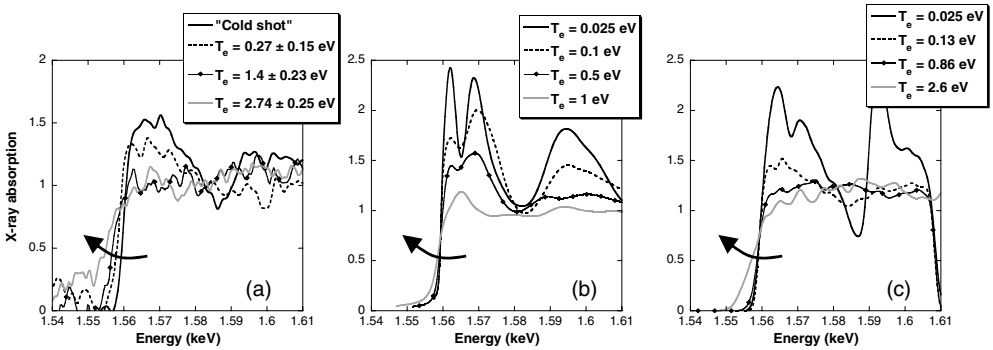

Figure 3. Al x-ray absorption spectra (normalized to the maximal mean value without XANES structures): (*a*) experimental measurements. (*b*) NPA-(M)HNC model. (*c*) *ab initio* QMD simulations. For clarity, we present in this figure only a chosen set of typical spectra. The 'cold shot' corresponds to a shot without heating proton beam. The similar calculated ones are for an electron temperature of 0.025 eV. The arrows in the figures highlight the smoothing of the slope with rising temperature.

thicknesses (0.47 and 1.6 μm). The probed surface has been estimated to be $170 \times 66\,\mu\text{m}^2$ on the Al sample plane, from the geometrical arrangement of the spectrometer and the x-ray source (5 mm behind the target in the Al sample/x-ray spectrometer axis).

Two other diagnostics, beyond the scope of this paper, were implemented on the experiment assigned to characterize the WDM sample. They consist of two-dimensional time-resolved optical self-emission [35] and surface expansion velocity through phase measurements of a reflecting probe beam [36].

3.2. XANES results

Controlling the delay between the two laser pulses, we recorded the absorption spectra after the proton heating of the sample ($\simeq$10 ps after the estimated initialization of the heating process).

Therefore, we consider that we probed the Al plasma at equilibrium, i.e. $T_\text{e} = T_\text{i}$, where T_e and T_i are, respectively, the electron and ion temperatures. Due to shot-to-shot fluctuations, the use of two different Al sample thicknesses and proton beam variations, we collected the XANES spectra for different temperatures. The resulting XANES experimental results are presented in figure 3(*a*).

We compared these results with two different theoretical approaches modelling the warm dense regime of matter. The resulting XANES spectra of these models described later are presented in figures 3(*b*) and (*c*) as a function of T_e.

On both the experimental and the calculated curves, we observe the Al K-edge followed by the XANES structures. With rising temperature, estimated with the help of a model described afterwards, the slope of the edge as well as the contrast of the XANES modulations are smoothed. The scope of the study presented in this paper is to interpret these observations.

4. Interpretation

To explain the structures observed in the absorption spectra, the starting point is the expression of the photoelectric cross section which is probed with this diagnostic [37]:

$$\sigma(E) \propto \sum_L |\langle \psi_{Lk} | \vec{\epsilon} \cdot \vec{r} | \phi_i \rangle|^2 \, (1 - f(E)) \, .$$

This expression is just a form of the Fermi–Golden rule. $\vec{\epsilon}$ is the x-ray polarization vector, $|\phi_i\rangle$ is a core state (1s for the K-edge), $|\psi_{Lk}$ (where $L \equiv (l, m)$) is a continuum state and $1 - f(E)$ is the occupation factor. According to this expression, the edge observed in the spectrum is related to the second term $1 - f(E)$ while the modulations of the absorption are included in the final state $|\psi_{Lk}\rangle$. The calculation of the latter is the principal objective of the theoretical models developed for describing this state of matter.

4.1. Theoretical models

These experimental data are compared with two different theoretical approaches to describe the WDM regime, which are, respectively, detailed in [38–40].

The first one describes the system through the neutral pseudoatom (NPA) concept [41, 42] which defines the elementary block of a model made of a core of bound electrons and a cloud of valence electrons. It gives an average calculation of the radial ion–ion correlation function $g(r)$ using (modified) hypernetted chain (HNC) equations (the term 'modified' comes from the addition of a so-called bridge function) and is a liquid-metal approach. Sampling the $g(r)$ function, the wave function of the photoelectron emitted during the x-ray photon absorption process is calculated. The photoionization cross section being directly related to this wave function, we deduce the absorption spectra. The second method is rather a solid state model based on electronic structure calculations. Here, we used *ab initio* quantum molecular dynamics simulations based on the density functional theory (DFT). This calculation provides a consistent set of properties ranging from dynamical (equation of states), electrical, optical to x-ray properties.

The absorption spectra resulting from these two models are presented in figures 3(b) and (c) for a sample of electron temperatures in the range of the experimental ones.

4.2. Electron temperature measurement

As illustrated by the theoretical absorption spectra presented in figures 3(b) and (c), the steepness of the Al K-edge is a function of T_e. To deduce the experimental electron temperature from this slope, we developed a model based on the Fermi–Dirac statistics giving a simplified representation of the x-ray photon absorption.

In a first approximation, probing the sample around the K-edge is equivalent to probing the unoccupied electronic density of states (DOS) ($\propto ||\psi_{Lk}\rangle|^2$) [24], proportional to $\sqrt{E}\,(1 - f(E))$, where $f(E) = 1/\left(e^{(E-\mu(T_e))/k_B T_e} + 1\right)$ is the Fermi–Dirac distribution function, E the x-ray photon energy and $\mu(T_e)$ the chemical potential. The term $\sqrt{E}$ comes from the DOS estimated for Al, which is a simple metal. However, due to the selection rules, we experimentally mainly probe the DOS of the p levels. Both calculated curves (total DOS and DOS projected on 'p' levels) by the use of the NPA-(M)HNC model for a cold cluster of 13 Al atoms in the fcc configuration are represented in figure 4(a). According to this result, the total DOS follows the $\sqrt{E}$ assumed behaviour. The p levels present a rather flat trend after the Al K-edge compared with the total DOS. Thereby, we choose to model the absorption spectra by the function $1 - f(E)$. We estimated $\mu(T_e)$ according to the Sommerfeld formula [43]. In figure 4(b), a sample of these curves for different T_e is reported.

Measuring the slope around the K-edge at the inflection point on these calculated curves for different T_e, we deduce a relation between the slope and the electron temperature. This relation was used to determine the experimental temperature of the WDM Al foil for each shot, reported in figure 3(a). According to this calculation, we heated the sample to a temperature in the range of a few electronvolts.

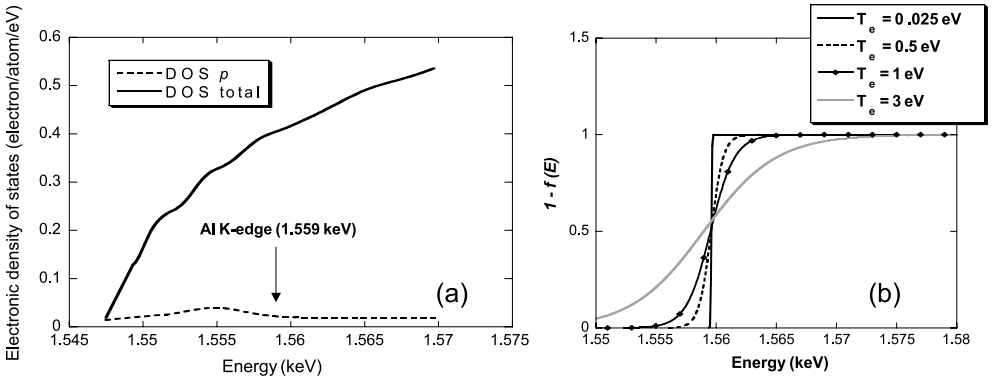

Figure 4. (*a*) Calculated density of states using NPA-(M)HNC model: total and projected on '*p*' levels. (*b*) $(1 - f(E))$ for different electron temperatures.

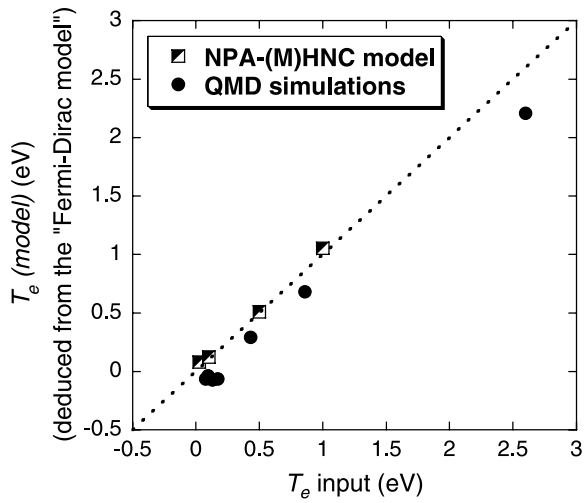

Figure 5. Comparison of the electron temperature deduced from the 'Fermi–Dirac model' T_e (model) with the T_e input in calculations. The dashed line represents the curve $T_e(\text{model}) = T_e$.

This estimation of the electron temperature was used, in a first attempt, to verify that the sample was probed in a solid density and homogeneous state. Taking into account a rough estimation of the temporal delay between the proton heating and the x-ray probing time, we determined the sample thickness Δd affected by the expansion. For this purpose, Δd is calculated considering the hydrodynamic expansion of the target at the ion-acoustic velocity ($c_s = \sqrt{Zk_B T_e/m_i}$). We excluded the shots following the criterion: $|\Delta d/d| > 10\%$ where d is the initial Al thickness. The spectra presented in figure 2(*a*) have been retained through this method.

Finally, we used the theoretical calculated curves presented in figures 3(*b*) and (*c*) to validate the rough 'Fermi–Dirac model' described here and that the provided T_e are a good evaluation of the experimental temperature. Thus, we applied the same analysis on the theoretical curves and compared the deduced temperature with the calculation inputs. According to figure 5, this method leads to a maximal error of 15%.

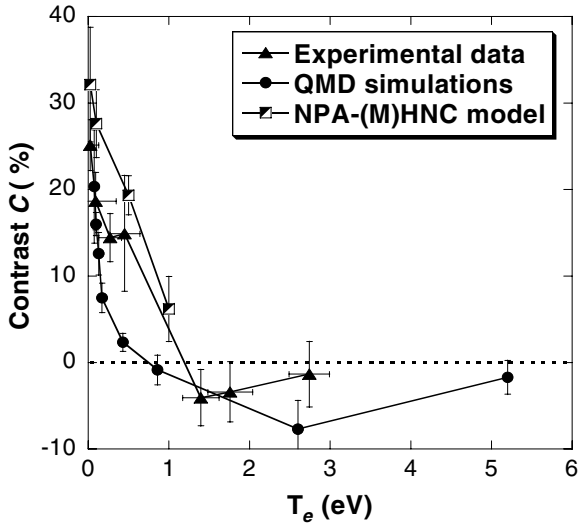

Figure 6. Experimental and calculated contrast of the XANES structures as a function of temperature. The error bars on T_e and C, are respectively, due to the accuracy of measuring the slope around the K-edge and the standard deviation calculating the average signals around XANES maximum and minimum (I_{max} and I_{min}).

4.3. Ion–ion correlation

In figure 3(*a*), one can clearly observe on the absorption spectra that the XANES structures progressively disappear when the electron temperature increases. We quantified such a trend by deducing from the experimental and theoretical absorption curves the contrast of the XANES structures, defined by $C = (I_{max} - I_{min})/(I_{max} + I_{min})$, where I_{max} and I_{min}, respectively, correspond to the average signal around the first XANES maximum ($\simeq$1.56–1.57 keV) and minimum ($\simeq$1.58–1.59 keV). The evolution of the contrast C, as a function of the electron temperature, is reported in figure 6. The experimental data are in good agreement with the calculated ones and the spectra are rather flat for a temperature around 1 eV.

These structures are related to the short-range order in the sample [24] and consequently to an ion–ion correlation loss due to heating. To support this interpretation, we represent in figures 7(*a*) and (*b*) the radial ion–ion correlation function $g(r)$ calculated using the two models we have mentioned before and for different T_e. Comparing both curves for a given temperature, the models are in good agreement. In both cases, the smoothing of the $g(r)$ function is significant for 1 eV which is related to the observed vanishing of the XANES structures.

5. Conclusions

In summary, we have developed a time-resolved diagnostic based on XANES using a laser-induced optimized x-ray source. This diagnostic has been used to probe a WDM Al sample heated by laser-produced proton burst in a single shot mode. In the studied situation, the sample was at equilibrium ($T_e = T_i$) with temperatures up to 3 eV. Analysing the absorption spectra, we extracted the temperature of the sample from the slope of the K-edge with an accuracy of 15%. In good agreement with two different theoretical approaches, we observe that the XANES structures are progressively smoothed when increasing the temperature up to

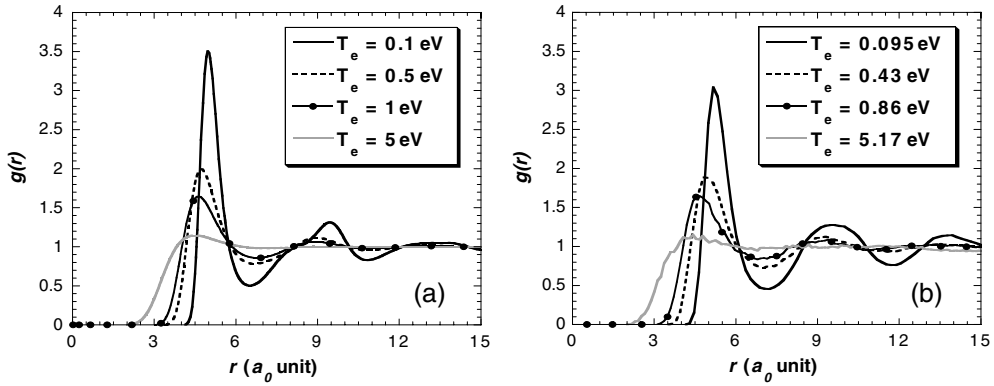

Figure 7. Radial ion–ion correlation function $g(r)$ as a function of temperature at solid density calculated with NPA-(M)HNC model (*a*) and *ab initio* QMD simulations (*b*). The distance r is reported in Bohr radius unit.

about 1 eV. Simulations demonstrate that this feature is directly related to a significant loss of ion–ion correlation.

This first experiment clearly validates the XANES as a diagnostic of the matter local structure and of the electron temperature. Thus, this study will be extended in future experiments to other materials and a wider panel of experimental conditions such as for example laser-shock compressed sample. In addition, we plan to take advantage of the high temporal resolution of this diagnostic ($\simeq$ps) to dynamically study the transition from solid to WDM before equilibrium ($T_e > T_i$), probing for example femtosecond laser-heated samples.

References

[1] Pfeifer T *et al* 2006 *Rep. Prog. Phys.* **69** 443
[2] Lee R W *et al* 2003 *J. Opt. Soc. Am.* B **20** 770
[3] Koenig M *et al* 2005 *Plasma Phys. Control. Fusion* **47** B441
[4] Car R and Parrinello M 1985 *Phys. Rev. Lett.* **55** 2471
[5] Perrot F and Dharma-wardana M W C 1987 *Phys. Rev.* A **36** 238
[6] Kohn W and Sham L J 1965 *Phys. Rev.* A **140** 1133
[7] Cavalleri A *et al* 2001 *Phys. Rev. Lett.* **87** 237401
[8] Rischel C *et al* 1997 *Nature* **390** 490
[9] Rousse A *et al* 2001 *Nature* **410** 65
[10] Sokolowski-Tinten K *et al* 2001 *Phys. Rev. Lett.* **87** 225701
[11] Lindenberg A M *et al* 2008 *Phys. Rev. Lett.* **100** 135502
[12] Garciá Saiz A *et al* 2008 *Phys. Rev. Lett* **101** 075003
[13] Glenzer S H *et al* 2007 *Phys. Rev. Lett.* **98** 065002
[14] Ravasio A *et al* 2007 *Phys. Rev. Lett.* **99** 135006
[15] Landen O L *et al* 2001 *J. Quant. Spectrosc. Radiat. Transfer* **71** 465
[16] Dobosz S *et al* 2005 *Phys. Rev. Lett.* **95** 025001
[17] Theobald W *et al* 1996 *Phys. Rev. Lett.* **77** 298
[18] Cavalleri A *et al* 2005 *Phys. Rev. Lett.* **95** 067405
[19] Yaakobi B *et al* 2008 *Phys. Plasmas* **15** 062703
[20] Audebert P *et al* 2005 *Phys. Rev. Lett.* **94** 025004
[21] Seres E *et al* 2006 *Appl. Phys. Lett.* **89** 181919
[22] Hall T A *et al* 1998 *Europhys. Lett.* **41** 495
[23] Bressler C and Chergui M 2004 *Chem. Rev.* **104** 1781
[24] Rehr J J and Albers R C 2000 *Rev. Mod. Phys.* **72** 621
[25] Forget P *et al* 2004 *Chem. Phys.* **299** 259

[26] Harmand M *et al* 2009 *Phys. Plasmas* **16** 063301
[27] Dorchies F *et al* 2008 *Phys. Rev. Lett.* **100** 205002
[28] Dorchies F *et al* 2008 *Appl. Phys. Lett.* **93** 121113
[29] Wilks S C *et al* 2001 *Phys. Plasmas* **8** 542
[30] Borghesi M *et al* 2004 *Phys. Rev. Lett.* **92** 055003
[31] Patel P K *et al* 2003 *Phys. Rev. Lett.* **91** 125004
[32] Snavely R A *et al* 2007 *Phys. Plasmas* **14** 092703
[33] Antici P *et al* 2006 *J. Phys. IV* **133** 1077
[34] Dyer G M *et al* 2008 *Phys. Rev. Lett.* **101** 015002
[35] Kodama R *et al* 1999 *Rev. Sci. Instrum.* **70** 625
[36] Mancic A *et al* 2009 *High Energy Density Phys.* submitted
[37] Peyrusse O 2009 *14th APS Topical Conf. on Atomic Processes in Plasmas*
[38] Peyrusse O 2008 *J. Phys.: Condens. Matter* **20** 195211
[39] Mazevet S and Zérah G 2008 *Phys. Rev. Lett.* **101** 155001
[40] Recoules V and Mazevet S *Phys. Rev.* B submitted
[41] Ziman J M 1964 *Adv. Phys.* **13** 89
[42] Perrot F 1990 *Phys. Rev.* A **42** 4871
[43] Ashcroft N W *et al* 2003 *EDP Sciences*